

PAPER • OPEN ACCESS

Hyperspectral camera based on a Fabry-Pérot with varying beam incidence

To cite this article: L Giovannelli *et al* 2017 *J. Phys.: Conf. Ser.* **841** 012003

View the [article online](#) for updates and enhancements.

Related content

- [Interference phenomenon obtained by replacing the two mirrors of a Michelson interferometer by Fabry-Pérot plates](#)
N Aebischer and P Bayat-Mokhtari
- [Indium phosphide all air-gap Fabry-Pérot filters for near-infrared spectroscopic applications](#)
A Ullah, M A Butt, S A Fomchenkov *et al.*
- [Species Distribution Model using Hyperspectral Data Application in Peatland, Central Kalimantan](#)
Muhammad Dayuf Jusuf



IOP | ebooks™

Bringing you innovative digital publishing with leading voices to create your essential collection of books in STEM research.

Start exploring the collection - download the first chapter of every title for free.

Hyperspectral camera based on a Fabry-Pérot with varying beam incidence

L Giovannelli, F Berrilli and D Del Moro

Università di Roma “Tor Vergata”, Via della Ricerca Scientifica, I-00133 Roma, Italy

Abstract.

Fabry-Pérot interferometers are commonly used as tunable filters in a variety of scientific fields. We here consider the use of a single Fabry-Pérot as a universal tunable filter in hyperspectral imaging applications, when it is necessary to recover image information of the scientific target at different wavelengths.

Fabry-Pérot are commonly used to scan small portions of the spectrum, defined by suitable prefilters. This is necessary due to the multi-peak response of a single interferometer. In order to overcome this issue we propose a novel triple-pass configuration, able to provide a fast and continuous sampling of the electromagnetic spectrum in the visible-infrared range without the need for a collection of dedicated prefilters.

1. Introduction

The ideal instrument for spectroscopy in a variety of scientific fields is a filter with a tunable centerband, which could cover a wide range of the electromagnetic spectrum, sampling light intensity at different wavelengths. Fabry-Pérot Interferometers (FPI) are commonly used as tunable filters in Astronomy (in ground based observatories i.e. VLT [1], Gemini [2], GTC [3], or in space missions i.e. Dynamic Explorer [4], JWST [5], Bepi-Colombo [6]), Information and Communications Technology [7, 8], Photonics [9–11], Atmospheric Physics [12–14] and other research fields.

FPIs have some major advantages with respect to long slit spectrographs:

- Fast response: can be tuned changing the spectral position in few ms. A full scan is completed in tens of seconds in the case of an FPI whereas can last minutes in the case of a long slit spectrograph.
- High transparency: given the same collecting area and the same spectral resolving power, the flux of light exiting an FPI can be 30 times the one exiting a long slit spectrograph [15].
- Adjustable: an FPI is not only tunable in wavelength at fixed step, you can program the portion of the spectrum you want to sample jumping by where it is not necessary to register the information. Furthermore, it is possible to vary the spectral resolving power in different portions of the spectrum.

The spectral response of a single FPI is a comb of peaks along the whole spectrum, which corresponds to different interference orders. The interference comb can be opportunely fine-shifted varying the optical cavity spacing. The goal of a FPI based instrument is to select just one interference order to obtain a nearly monochromatic signal. For this reason an FPI is always used



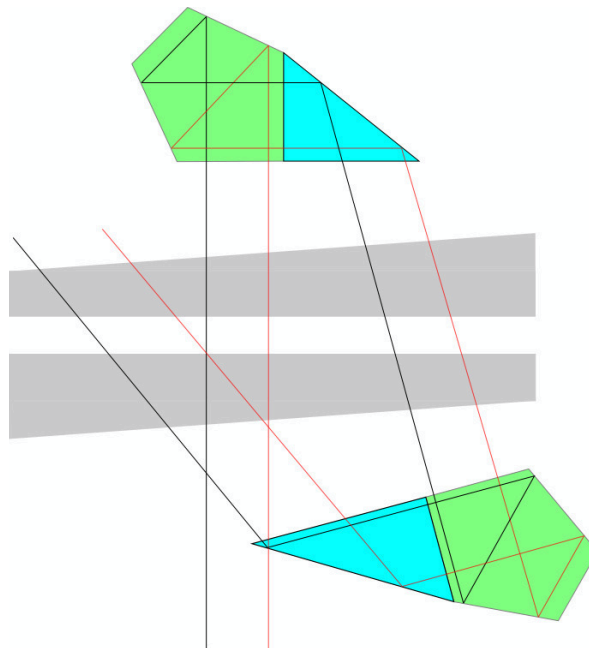


Figure 1. Optical layout. The FPI (gray) is seen from above. As usual to avoid unwanted ghost reflections from the external optical surfaces, the optical plates are wedged. The pentaprisms (light green) collect the beam and provide a 90 degree reflection. The inclination angle is set by the prisms (light blue), optically contacted with the pentaprisms. Two rays of the optical beam are shown in red and black. The superposition of the reflected beam is avoided due to a suitable arrangement in 3D.

with a prefilter to select the portion of the spectrum to be investigated. For a more comprehensive description of single FPI see e.g. [16–20]. This may be not sufficient since the bandwidth of the prefilter is often much greater than the Free Spectral Range (FSR), i.e. the distance between two subsequent peaks of the FPI comb. The solution is often to use two or more FPIs in series, with slightly different FSR to obtain the superposition of just one transparency peak in the prefilter bandwidth (see e.g. [21, 22]). We here propose for the first time a different solution using just one FPI in an triple pass configuration, with a varying beam incidence, to obtain an extended FSR (see Fig. 1). The result is a compact instrument which is here proposed as a universal tunable filter.

We report here just a few examples of scientific cases in which an FPI could be an improvement compared to nowadays instruments:

- Earth observation from satellites. Hyperspectral datasets are used, for example, to distinguish terrain characteristics and the type of cultivation. See i.e. the datasets provided by AVIRIS satellite, which uses 224 spectral channels with contiguous 10 nm sampling from 400 nm to 2500 nm [23].
- Archaeological and arts applications. Hyperspectral cameras are used e.g. to reveal hidden features in paintings and artifacts in reflectometry when X-rays and IR techniques fails [24]. In this case 1000 partially overlapped bands of 2.5 nm in the visible and near-infrared region were used.
- Planetary surface mapping. We here focus in particular on imaging spectroscopy instruments used on different planetary missions to understand chemical composition of the

soil and the atmosphere as well as the morphological evolution of planets and minor bodies of the Solar System [25,26]. E.g. CRISM is an imaging spectrometer with a scannable field of view that can cover wavelengths from $0.362 \mu\text{m}$ to $3.92 \mu\text{m}$ at $6.55 \text{ nanometers/channel}$ (~ 500 channels).

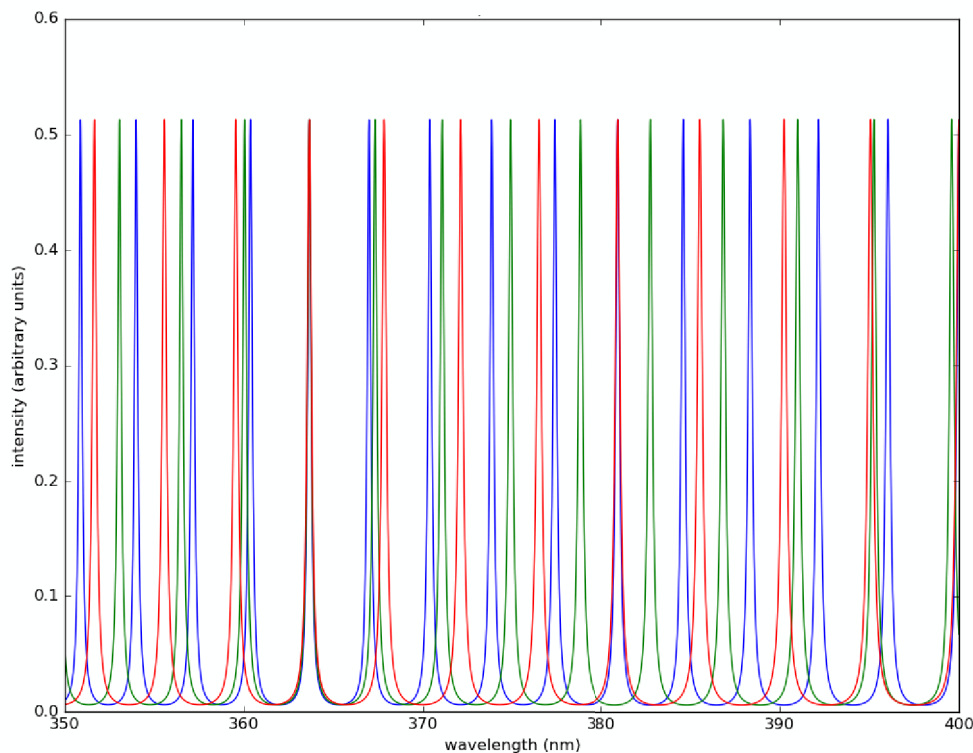


Figure 2. We show the simulation of the FPI spectral profile with three different angle of incidence. The first passage in the optical cavity (blue) has $\theta_1 \simeq 0$ to maximize the interference order and so spectral resolution. The second passage (green) has $\theta_2 \simeq 17.75$ in order to have a green peak superposed with a blue one every 20 green peaks. The third passage (red) has $\theta_3 \simeq 36.87$ in order to have a red peak superposed with a blue one every 4 red peaks. The incoming intensity is set to 1 all over the spectrum (a.u.).

2. The new design with varying incidence angle

Usually a double or triple FPI configuration is used to extend the FSR of the instrument. Using different optical cavity spacing (OCS) every FPI is characterized by a different interference order $m = \frac{2n}{\lambda} d \cos \theta$, where n is the refractive index of the air, λ is the wavelength of interest, d is the OCS and θ is the angle of incidence of the beam respect to the optical surface normal. The FSR depends on the interference order: $FSR = \lambda/m$. Combining the spectral profiles together, it is possible to extend the FSR. We here propose the same effect with a single cavity. This is possible because we vary the incidence angle of the beam instead of d . We impose $FSR_2 = 1.05 FSR_1$ and $FSR_3 = 1.25 FSR_1$ in order to have one coincident peak out of 20 in the first case and one out of 4 in the second (see Fig. 2). We impose $\theta_1 = 0$ to maximize the interference

order and so spectral resolution. From FSR calculation we get: $\theta_2 \simeq 17.75^\circ$ and $\theta_3 \simeq 36.87^\circ$. This geometric configuration is obtained using a pentaprism optically contacted with a prism with a suitable angle to fine tune the new incidence angle of the beam (see Fig. 1). This optical configuration guarantees the same inclination angle even in the case of minor misalignments of the optical elements.

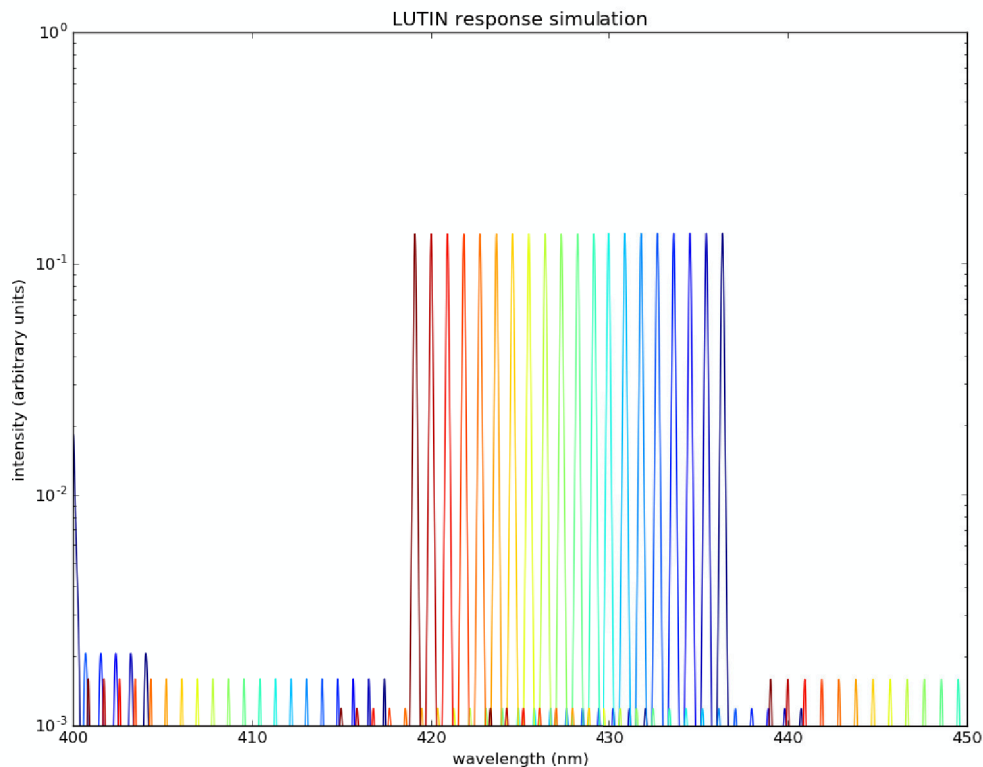


Figure 3. We show the simulation of the spectral profile after all three passages in the optical cavity. The different colours represent different steps during an FPI scan of the visible spectrum. Apart from weak secondary peaks, there is only one peak in the reported 50 nm portion of the spectrum. We set to 50 nm the variation of the optical cavity spacing, resulting in a spectral step of $\simeq 0.9$ nm, while the FWHM $\simeq 0.2$ nm. The incoming intensity is set to 1 all over the spectrum (a.u.).

We present the simulation for a FPI with an OCS of $24 \mu\text{m}$ in the range $400 \div 450\text{nm}$. The simulation take into account the effective finesse of a non-ideal FPI as in [17], using, as an example, the same parameters of the LUTIN prototype as in [20]. For a single pass, the resulting FWHM is $\simeq 0.8$ nm while the FSR $\simeq 3.5$ nm. With the triple pass the FSR around 400 nm is extended to ~ 80 nm, while around 800 nm is ~ 300 nm. The spectral purity of the instrument is high in the extended FSR region, as the contribution from secondary peaks is $< 4\%$. In this way it is possible to use standard broadband filters as pre-filters, like Johnson UBVRI filters, covering with a single FPI the whole VIS-NIR spectrum. We show in Fig. 3 the spectral profiles for every incidence angle, the combined spectral profile and a scan sequence with a 50 nm optical cavity scanning step. The effect of the inclination over the reflectivity of

the coatings is not taken into account here, since is highly dependent on the type of coating used in FPI outer and inner optical surfaces. However a preliminary calculus suggest that the final peak transparency of the FPI in the proposed inclined configuration must be $\sim 70\%$ respect to the case of three FPIs in series. Further investigation on this point will be performed once the technique will be applied to a specific real case. We stress that the three spectral profiles remain tuned during the scan, with only one parameter to be controlled, while a triple FPI system needs three cavity gaps to be tuned in sincro during the scan. Furthermore, given that the three inclination angles are fixed, the polarization induced by the reflection on the inclined optical surfaces can be easily taken into account by usual polarization calibration routines anyhow used in spectropolarimeters based on FPIs (see i.e. [27]).

3. Conclusions

In recent years, many imaging spectroscopy instruments have flown on different planetary missions, e.g. VIMS on Cassini, CRISM on Mars Reconnaissance Orbiter (MRO), and hyperspectral remote sensors from there have provided the measures that allowed us to understand the formation and evolutionary processes planets and minor bodies have undergone, through the surface mapping and composition study and the identification of specific surface features. In fact, hyperspectral imaging instruments play a major role in most of the planetary missions. The new instrument concept introduced in this work is a change of paradigm, since it provides imaging at a wavelength of choice, with a < 1 nm bandpass, in a very wide spectral range. These capabilities can be either exploited to reduce the amount of data to be acquired, processed and transmitted back, or to increase the data acquisition rate, or to tune the spectral sampling to the observation necessities. The flexibility of this instrument is such that it can play both the high-cadence imaging camera role when telemetry allows, and, at large distances from Earth, it can limit the data volume that has to be transmitted to the bare minimum, by selecting only the most interesting wavelengths.

References

- [1] Hartung M *et al.* 2004 *Society of Photo-Optical Instrumentation Engineers (SPIE) Conference Series* **5492**
- [2] Scott A *et al.* 2006 *Society of Photo-Optical Instrumentation Engineers (SPIE) Conference Series* **6269**
- [3] Cepa J *et al.* 2003 *Society of Photo-Optical Instrumentation Engineers (SPIE) Conference Series* **4841**
- [4] Killeen T L *et al.* 1983 *Applied Optics* **22** 22
- [5] Yoshikawa I *et al.* 2010 *Planetary and Space Science* **58** 1-2
- [6] Doyon R *et al.* 2008 *Society of Photo-Optical Instrumentation Engineers (SPIE) Conference Series* **7010**
- [7] Chan L Y *et al.* 2002 *Electronics Letters* **38** 1
- [8] Vahala K J *et al.* 2003 *Nature* **424**
- [9] Villatoro J *et al.* 2009 *Optics letters* **34** 16
- [10] Murphy K A *et al.* 1991 *Optics letters* **16** 4
- [11] Wu C *et al.* 2011 *Optics letters* **36** 3
- [12] Rees D *et al.* 1996 *Journal of Atmospheric and Terrestrial Physics* **58** 16
- [13] Xia H *et al.* 2007 *Applied Optics* **46** 29
- [14] Arshinov Y *et al.* 2005 *Applied Optics* **44** 17
- [15] Hernandez G 1988 *Fabry-Perot interferometers Cambridge University Press*
- [16] Berrilli F *et al.* 2011 *Society of Photo-Optical Instrumentation Engineers (SPIE) Conference Series* **8148**
- [17] Giovannelli L *et al.* 2012 *Society of Photo-Optical Instrumentation Engineers (SPIE) Conference Series* **8446**
- [18] Giovannelli L *et al.* 2012 *Journal of Physics Conference Series* **383**
- [19] Giovannelli L *et al.* 2014 *Society of Photo-Optical Instrumentation Engineers (SPIE) Conference Series* **9147**
- [20] Giovannelli L *et al.* 2014 *Journal of Physics Conference Series* **566**
- [21] Cavallini F 2006 *Solar Physics* **236** 415
- [22] Tritschler A Schmidt W Langhans K & Kentischer T 2002 *Solar Physics* **211** 17
- [23] Clevers J G P W 1999 *ISPRS Journal of Photogrammetry and Remote Sensing* **54** 299
- [24] Snijders L Zaman T & Howell D 2016 *Journal of Archaeological Science: Reports* **9** 143
- [25] Brown R H Baines K H Bellucci G *et al.* 2004 *Space Science Reviews* **115** 111

- [26] Murchie S Arvidson R Bedini P *et al.* 2007 *Journal of Geophysical Research (Planets)* **112** E05S03
- [27] Viticchié *et al.* 2010 *The Astrophysical Journal* **723** 1